



A Smooth Path Tracking Algorithm for Wheeled Mobile Robots with Dynamic Constraints

K. C. KOH

Division of Mechanical and Control Engineering, Sun Moon University, 100 Kalsanri, Asanshi, Chungnam-Do, 336-840, Korea; e-mail: kckoh@omega.sunmoon.ac.kr

H. S. CHO*

Department of Mechanical Engineering, KAIST, 373-1 Kusong, Yusong, Taejeon, 305-701, Korea; e-mail: hscho@lca.kaist.ac.kr

(Received: 25 April 1997; accepted: 28 August 1998)

Abstract. In order to avoid wheel slippage or mechanical damage during the mobile robot navigation, it is necessary to smoothly change driving velocity or direction of the mobile robot. This means that dynamic constraints of the mobile robot should be considered in the design of path tracking algorithm. In the study, a path tracking problem is formulated as following a virtual target vehicle which is assumed to move exactly along the path with specified velocity. The driving velocity control law is designed basing on bang-bang control considering the acceleration bounds of driving wheels. The steering control law is designed by combining the bang-bang control with an intermediate path called the landing curve which guides the robot to smoothly land on the virtual target's tangential line. The curvature and convergence analyses provide sufficient stability conditions for the proposed path tracking controller. A series of path tracking simulations and experiments conducted for a two-wheel driven mobile robot show the validity of the proposed algorithm.

Key words: steering control, bang-bang control, nonholonomic constraints, path tracking algorithm, motion planning, mobile robot navigation.

1. Introduction

In the navigation of the wheeled mobile robots, the slippage of the wheels is the crucial problem. To avoid it, the dynamic constraints such as the wheel acceleration bound should be considered in the design of the path planner or path tracking controller [3]. In the path planning, many authors' works had been studied on the design of a smooth curve with curvature continuity [7, 15] and optimality [23]. Since the mobile robot moves in uncertain environments, the path is often modified and the path error occurring during the navigation is compensated by the path tracking controller. However, there had been little effort on the design of the path tracking controller considering the motion smoothness or the dynamic constraints. The researchers had focused on guaranteeing the stability of the nonholonomic

* Corresponding author.

system [2, 8, 12, 14]. The detail state of arts is summarized below and in the following section the idea of the paper is presented.

1.1. PREVIOUS STUDIES

The control system of autonomous mobile robots generally comprises a path planner and a path tracking controller. The path error in the robot navigation primarily depends on the smoothness of the reference path given in the planning stage. The various path planning methods using a smooth curve satisfying the curvature continuity have been addressed in the previous works [7, 15, 16, 19, 25]. The works include the clothoid pair method [15], polynomial curve method [7, 16, 19, 25] and time-optimal trajectory planning [23]. These methods, however, require too much computational effort to be implemented in real time. Furthermore, there exist geometric limitations on the boundary conditions that the curve should be functionally given at any configuration. Thus, the path is often given by combinations of line or arc segments in the environment with obstacles. However, such a path causes large path error or abrupt motion due to the dynamic constraints inherent to the mobile robot. The transient motion trajectory towards the path from the deviated position depends on the path tracking algorithm.

The previous works on the path tracking controller can be classified into the following four categories: linear [4, 5, 21], nonlinear [1, 2, 10–12, 15], geometrical [6, 8, 24, 26] and intelligent [9] approaches. The linear approaches are computationally simple, but the path tracking motion is inconsistent with size of the path errors. To cope with the problem, several authors have proposed nonlinear path tracking algorithms. Those include a path tracking method based on the Lyapunov function [12, 15], and a nonlinear steering control law [11] considering the driving speed. The nonlinear approaches, however, consider only path error convergence or system stability, but neglect the smoothness of the transient trajectory or dynamic constraints. The geometric approaches are regarded as attempts to connect the path tracking to path planning. Singh et al. [24] have proposed the so-called quintic polynomial method in which the fifth order polynomial curve is designed under six boundary conditions. Tsugawa [26] has presented a target point following algorithm in which a cubic spline curve is used to determine the steering angle or rotational velocity of the robot. These geometric schemes show the smooth tracking motion to guide the mobile robot towards the reference path, but neglect the dynamic constraints, such as the curvature or acceleration limits which are important factors for avoiding wheel slippage or mechanical shock during the navigation.

1.2. OVERVIEW OF THE PAPER

In this paper, we propose a smooth path tracking algorithm considering the dynamic constraints such as bounds on wheel velocities and accelerations. By introducing the concept of the virtual target vehicle, the path tracking control is

formulated as a target following problem. In the scheme, the driving velocity and steering control laws are independently designed based on a bang-bang control algorithm. To cope with the nonholonomic constraints, the steering control law is driven by employing an on-line design of the landing curve so that the robot can get back smoothly towards the target direction. By Lyapunov's direct method, the convergence of the path error is analyzed and the condition for the landing curve parameter is given from curvature analysis. To show the validity of the proposed algorithm, a series of path tracking simulations and experiments were conducted for a prototype mobile robot with differential wheels. The results demonstrate that the proposed algorithm provides a quick and smooth tracking performance with practical implementation.

The paper is organized as follows: Section 2 describes the kinematic characteristics of a two-wheeled mobile robot with a concept of virtual target vehicle. Section 3 presents the proposed path tracking algorithm, Section 4 discusses path tracking simulation results, and concluding remarks are given in Section 5.

2. Problem Statement

2.1. KINEMATICS OF A TWO-WHEELED MOBILE ROBOT

Let us consider a mobile robot driven by two differential wheels as shown in Figure 1. The center of motion, denoted by C , is located at the midpoint between the left and right driving wheels. Assuming that the robot moves on the planar surface without slipping, the tangential velocity v_c and angular velocity ω_c at the center C can be written as

$$v_c = \frac{r_w}{2}(\omega_r + \omega_l), \quad (1)$$

$$\omega_c = \frac{r_w}{d_w}(\omega_r - \omega_l), \quad (2)$$

where ω_r and ω_l denote the rotational velocities of the right and left driving wheels, respectively, r_w is the radius of the wheels, and d_w is the azimuth length between the wheels. The kinematic equation of the mobile robot is given by

$$\dot{x}_c = v_c \cos(\theta_c), \quad (3)$$

$$\dot{y}_c = v_c \sin(\theta_c), \quad (4)$$

$$\dot{\theta}_c = \omega_c, \quad (5)$$

where coordinates (x_c, y_c) indicate the position of the robot with respect to the world coordinate system and θ_c is the heading angle of the robot. The triplet (x_c, y_c, θ_c) is used for defining the robot posture and represented by vector \mathbf{P} . The posture of the robot can be estimated from integration of Equations (3)–(5). The integration is implemented by the following iterative algorithm called dead reckoning:

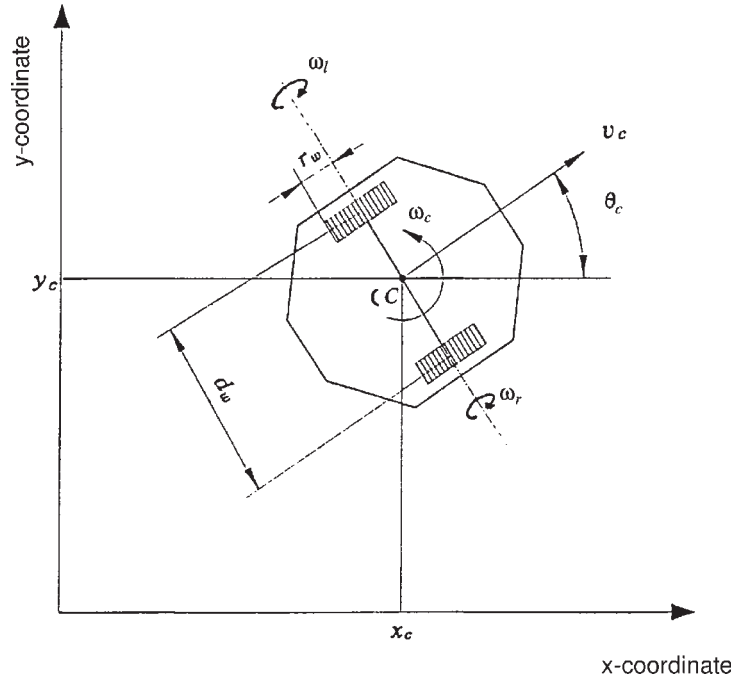


Figure 1. Definitions of posture and velocities of a two-wheeled mobile robot.

(i) in case $\omega_c \neq 0$

$$x_c^{k+1} = x_c^k + \frac{v_c}{\omega_c} [\sin(\theta_c^{k+1}) - \sin(\theta_c^k)], \quad (6)$$

$$y_c^{k+1} = y_c^k - \frac{v_c}{\omega_c} [\cos(\theta_c^{k+1}) - \cos(\theta_c^k)], \quad (7)$$

$$\theta_c^{k+1} = \theta_c^k + \omega_c t_s, \quad (8)$$

(ii) in case $\omega_c = 0$

$$x_c^{k+1} = x_c^k + v_c t_s \cos(\theta_c^k), \quad (9)$$

$$y_c^{k+1} = y_c^k + v_c t_s \sin(\theta_c^k), \quad (10)$$

$$\theta_c^{k+1} = \theta_c^k, \quad (11)$$

where k denotes the sampling index and t_s is the sampling time.

2.2. DYNAMIC CONSTRAINTS

Any abrupt change in the robot motion may cause the slippage or mechanical damage to the mobile robot. If the angular acceleration of each driving wheel is limited by $\dot{\omega}_{\max}$

$$|\dot{\omega}_{r,l}| \leq \dot{\omega}_{\max} \quad (12)$$

then, from (1) and (2), the tangential and angular accelerations of the robot are bounded by

$$|a_c| + \frac{d_w}{2} |\alpha_c| \leq r_w \dot{\omega}_{\max}. \quad (13)$$

The above equation means that the maximum allowable bounds on tangential and angular accelerations of the robot are coupled with each other. The ranges of each value to be independently considered are obtained by taking half the value of each maximum as

$$|a_c| \leq a_{\max} = \frac{r_w \dot{\omega}_{\max}}{2}, \quad (14)$$

$$|\alpha_c| \leq \alpha_{\max} = \frac{r_w \dot{\omega}_{\max}}{d_w}, \quad (15)$$

where a_{\max} and α_{\max} are the tangential and angular acceleration limits of the robot, respectively.

2.3. TARGET VEHICLE AND PATH ERROR

To define path error in time domain, we introduce the virtual target vehicle which is assumed to ideally move along the given path. The motion of the target vehicle can be represented by target posture \mathbf{P}_t and target velocity vector \mathbf{V}_t at the sampling time k , given by

$$\mathbf{P}_t(k) = [x_t(k), y_t(k), \theta_t(k)]^T, \quad (16)$$

$$\mathbf{V}_t(k) = [v_t(k), \omega_t(k)]^T. \quad (17)$$

The tangential and angular velocities of the target vehicle v_t and ω_t are determined by

$$v_t(k) = v_p^i, \quad (18)$$

$$\omega_t(k) = \kappa_p^i v_p^i, \quad (19)$$

where v_p^i and κ_p^i are the specified driving speed and curvature on the i th path segment, respectively. The current motion of the robot can be represented by the current posture \mathbf{P}_c and current velocity vector \mathbf{V}_c as

$$\mathbf{P}_c(k) = [x_c(k), y_c(k), \theta_c(k)]^T, \quad (20)$$

$$\mathbf{V}_c(k) = [v_c(k), \omega_c(k)]^T, \quad (21)$$

and computed via previously described dead reckoning. For notational simplicity, the indices of the sampling interval k will be omitted or superscript hereafter. The path error is defined in the local coordinate with respect to the target vehicle as

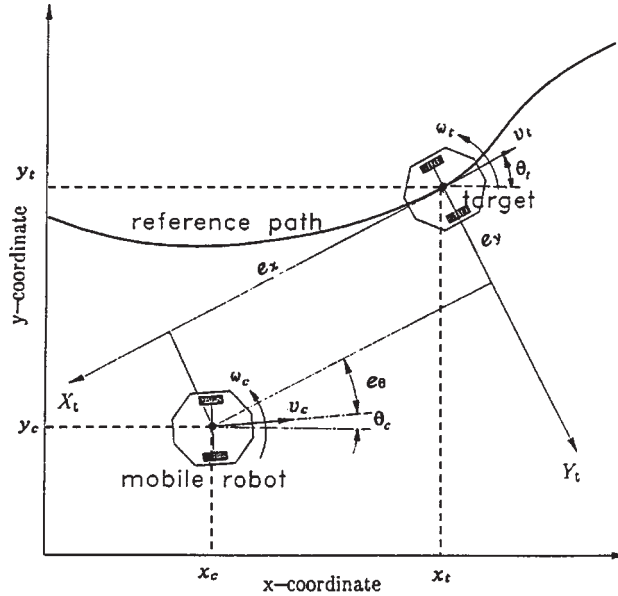


Figure 2. Virtual target and path error defined in the local target coordinate system.

shown in Figure 2 and can be represented by

$$e_x = (x_t - x_c) \cos(\theta_t) + (y_t - y_c) \sin(\theta_t), \quad (22)$$

$$e_y = (x_t - x_c) \sin(\theta_t) + (y_t - y_c) \cos(\theta_t), \quad (23)$$

$$e_\theta = \theta_t - \theta_c, \quad (24)$$

where e_x and e_y are called *tangential* and *lateral path errors*, respectively, and e_θ is called *angular path error*. Using the concept of the virtual target, we can reformulate the path tracking problem as the target following problem in which the mobile robot tracks the virtual target vehicle. The target vehicle can start from any initial posture and make discontinuous tangential and angular motions crossing over the boundaries of path segments, while the robot subjects to dynamic constraints during the tracking motion. Thus, the path error mainly arises from this difference in dynamics.

3. The Proposed Path Tracking Algorithm

3.1. TIME OPTIMAL BANG-BANG CONTROL

Before going into the proposed tracking algorithm, let us consider a bang-bang control for a double integrator system represented by

$$\dot{x}_c = v_c, \quad (25)$$

$$\dot{v}_c = a_c, \quad (26)$$

where x_c , v_c and a_c are position, velocity, and acceleration of the vehicle, respec-

tively. The system input is the acceleration and output is the position. When the acceleration a_c is bounded by (14), the control law of determining a_c so that this system reach the target position x_t and velocity v_t in minimum time is the bang-bang control given by

$$v_s = v_t - v_c + [2a_{\max}|x_t - x_c|]^{1/2} \text{sgn}(x_t - x_c), \quad (27)$$

$$a_c = a_{\max} \text{sgn}(v_s), \quad (28)$$

where v_s is a switching condition and $\text{sgn}(\cdot)$ is the sign operator. The law can be digitally implemented by modifying the switching rule of (28) to avoid the limit cycle due to the finite sampling interval of ΔT

$$a_c = \mu(v_s/\Delta T, a_{\max}), \quad (29)$$

where $\mu(a, b)$ is a clamping function defined by

$$\mu(a, b) = \begin{cases} a & \text{for } |a| < b, \\ b & \text{for } |a| \geq b. \end{cases} \quad (30)$$

3.2. PROPOSED PATH TRACKING METHOD

Now, let us consider the extension of the bang-bang control law to the tracking control of the two-wheel driven mobile robot moving on the plane kinematics of which is given by Equations (3)–(5). Due to the nonlinear and nonholonomic characteristics of the robot kinematics, it is very difficult to get the bang-bang action determining the wheel accelerations [23]. To meet the condition given by (14) and (15), it will be effective to design a path tracking controller based on bang-bang in spite of the difficulty in its direct extension. To cope with the conflict between the difficulty in direct extension and the use of bang-bang, we introduce a landing curve as an intermediate path proving the heading angle and angular velocity, values of which are required such that the mobile robot could softly land on the target line. The idea comes from the flight landing situation in which the heading angle and its rate in change are determined according to the height so as to safely land on the ground.

The proposed target tracking algorithm is composed of two independent laws: steering control and driving velocity control laws. Considering the dynamic constraints of (14) and (15), the above bang-bang control scheme is used to determine each velocity. Let us first consider the steering control law based on the landing curve.

3.2.1. Steering Control Law

The lateral path error e_y , the angular path error e_θ , and the angular velocity error $\omega_t - \omega_c$ between the robot and the target vehicle should be eliminated by the steering control law determining the angular velocity command of the robot, ω_c^{k+1} in the

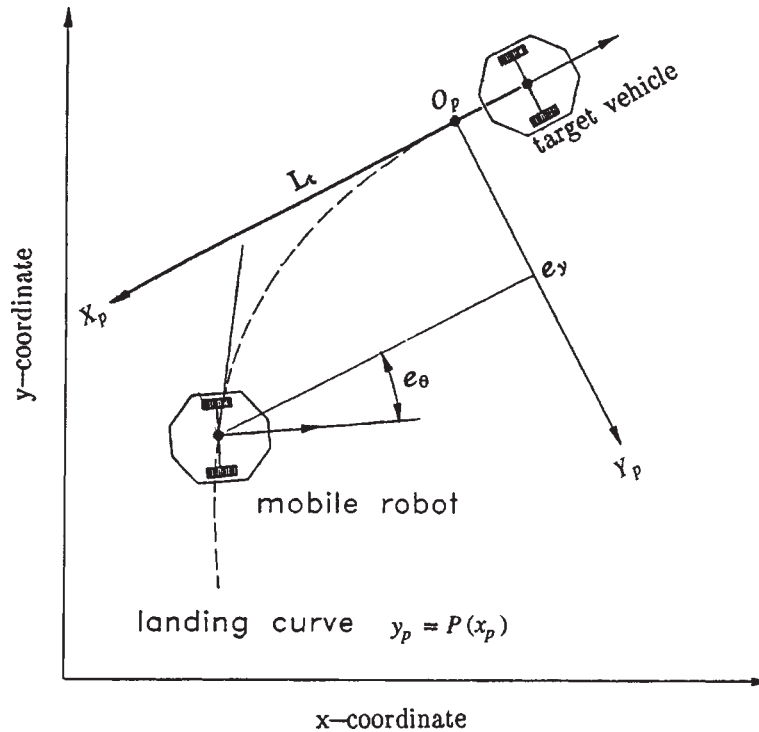


Figure 3. Landing curve design based on the tangential axis of the target coordinate.

next sampling time. First, the landing curve is designed as shown in Figure 3. Its origin O_p is on the target line L_t , direction of the target vehicle and the landing curve passes the center of the robot. If a local coordinate $(X_p - Y_p)$ at point O_p is defined, then the landing curve is selected by a polynomial function given by

$$y_p = P(x_p). \quad (31)$$

This curve satisfies the following boundary conditions to provide the continuities of the position, angle, and curvature at its origin, the landing point on the target line L_t :

$$P(x_p)|_{x_p=0} = 0, \quad (32)$$

$$\left. \frac{dP(x_p)}{dx_p} \right|_{x_p=0} = 0, \quad (33)$$

$$\left. \frac{d^2P(x_p)}{dx_p^2} \right|_{x_p=0} = 0. \quad (34)$$

The minimal order solution for above conditions becomes

$$P(x_p) = \pm c_x x_p^3, \quad (35)$$

where c_x is a positive constant denoting the *landing coefficient*. The sign of the curve is determined according to the sign of lateral path error e_y

$$P(x_p) = c_x x_p^3 \text{sgn}(e_y). \quad (36)$$

From Equation (36), the tangential angle θ_p of the landing curve and its differential $\dot{\theta}_p$ can be calculated at the center of the robot

$$\theta_p = \theta_t + \tan^{-1} \left[3c_x \left(\frac{e_y}{c_x} \right)^{2/3} \text{sgn}(e_y) \right], \quad (37)$$

$$\omega_p = \dot{\theta}_p = \omega_t + \frac{2(e_y/c_x)^{-1/3}}{1 + \tan^2(\theta_p - \theta_t)} \dot{e}_y \text{sgn}(e_y), \quad (38)$$

where \dot{e}_y can be obtained from differentiation of Equation (23),

$$\dot{e}_y = -\omega_t e_x + v_c \sin(e_\theta). \quad (39)$$

Now, the bang-bang control scheme can be directly applied to the angular velocity control law since the landing angle θ_p and its change ω_p become the target angle and target angular velocity to be followed at the current posture:

$$\omega_s = \omega_p + \{2\alpha_{\max} |\theta_p - \theta_c|\}^{1/2} \text{sgn}(\theta_p - \theta_c), \quad (40)$$

$$\alpha_c = \mu \frac{\omega_s}{\Delta T}, \alpha_{\max}, \quad (41)$$

$$\omega_c^d(k+1) = \omega_c(k) + \alpha_c \Delta T. \quad (42)$$

The path error convergence will be discussed in Appendix B. The landing coefficient c_x has some effect on the tracking performance since its large value leads to steep curvature of the landing curve. Figures 4(a) and (b) show this effect. The large value of c_x will improve the convergence rate of the tracking motion but its bound should be considered with the dynamic constraints of the robot. The curvature equation of curves defined in Cartesian coordinates is given by

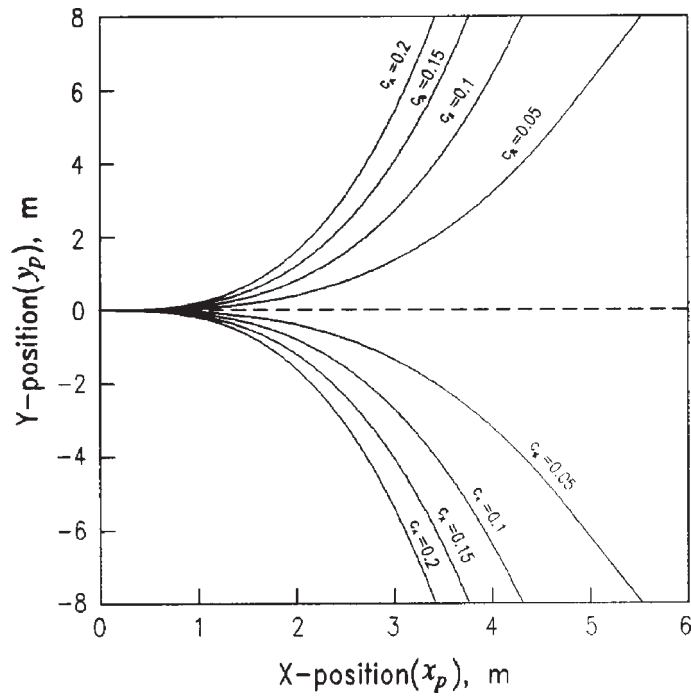
$$\kappa(x) = \frac{d^2 y / dx^2}{\{1 + (dy/dx)^2\}^{3/2}}, \quad (43)$$

where $\kappa(x)$ is the curvature. Substituting the landing curve equation $y = c_x x^3$ into Equation (43) yields

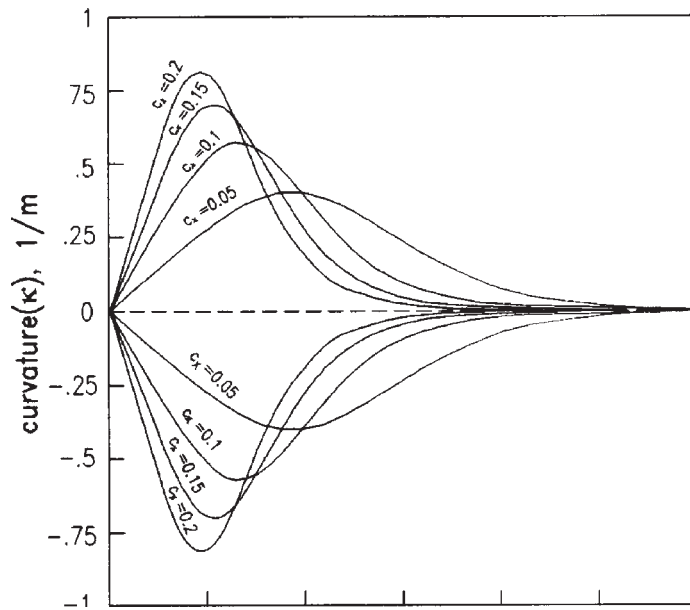
$$\kappa(x) = \frac{6c_x x}{(1 + 9c_x^2 x^4)^{3/2}}. \quad (44)$$

As shown in Figure 4(b), the change rate of curvature increases as the landing coefficient becomes larger and has a maximum value at the origin. From this fact, we can compute the maximum value as

$$\dot{\kappa}_{\max} = \left. \frac{d\kappa(x)}{dt} \right|_{x=0} = 6c_x v_t \quad (45)$$



(a) landing curve variation



(b) curvature variation

Figure 4. Variations of landing curves and curvatures according to different landing coefficients: (a) landing curve variation; (b) curvature variation.

and connecting it to the angular acceleration bound of Equation (15) with a condition of $\dot{\omega}_t = 0$,

$$\dot{\kappa}_{\max} < \alpha_{\max}/v_t. \quad (46)$$

From Equations (45) and (46), the limit condition for c_x can be obtained by

$$c_x < \frac{\alpha_{\max}}{6v_t^2}. \quad (47)$$

Hence, the landing coefficient c_x can be properly determined under the condition of (47). Note that Equation (47) implies the conditions of constant tangential and angular velocities, $\dot{v}_t = \dot{\omega}_t = 0$ which are valid in the path planning with straight or circular path segments.

3.2.2. Driving Velocity Control Law

Compared to the steering control law, the driving velocity control law can be derived in a simple manner. Assuming the orientation to be aligned by the steering control law, the tangential path error e_x and its rate in change can be directly the target values of the driving controller, determining the tangential velocity of the robot, v_c^{k+1} in the next sampling time. The rate of change in e_x with respect to time is computed from differentiation of Equation (22),

$$\dot{e}_x = v_t - v_c \cos(e_\theta) + \omega_t e_y. \quad (48)$$

Then, basing on these tangential path and velocity errors, the tangential velocity control law is derived as follows:

$$v_s = \dot{e}_x + [2a_{\max}|e_x|]^{1/2} \text{sgn}(e_x), \quad (49)$$

$$a_c = \mu \left(\frac{v_s}{\Delta T}, a_{\max} \right), \quad (50)$$

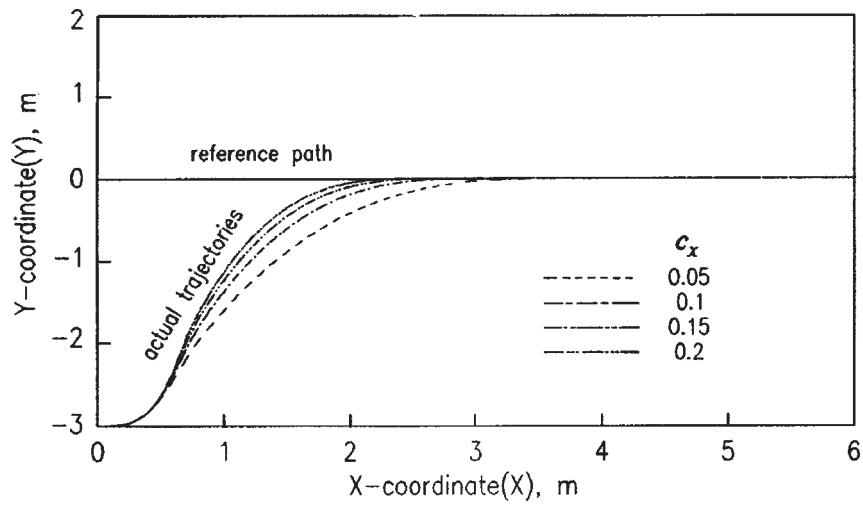
$$v_c^{k+1} = v_c^k + a_c \Delta T. \quad (51)$$

4. Simulations and Experiments

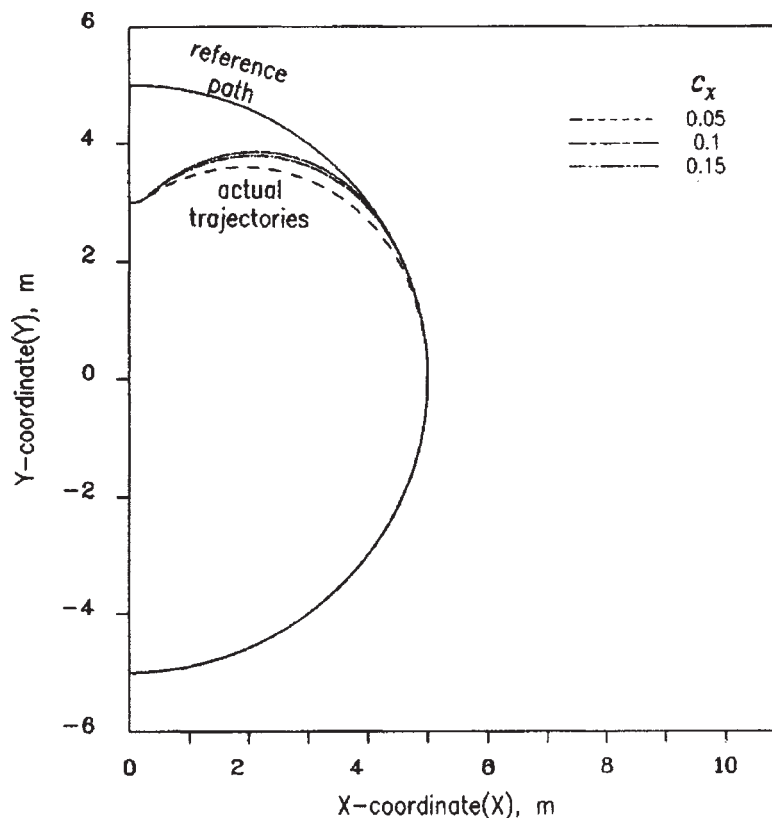
4.1. COMPUTER SIMULATION

Before experiments, a series of path tracking simulations was conducted to investigate the performance of the proposed path tracking algorithm under various conditions. In the simulation, we used the following parameters for dynamic constraints: $a_{\max} = 0.3 \text{ m/sec}^2$ and $\alpha_{\max} = 1.2 \text{ rad/sec}^2$, and for various values of $c_x = 0.05, 0.1, 0.15$ and 0.2 . Figure 5(a) shows the path trajectories obtained by performing the tracking motion for a straight line under the following condition:

- (i) target velocity: $v_t(0) = 1 \text{ m/sec}$, $\omega_t(0) = 0 \text{ rad/sec}$,
- (ii) initial error posture: $e_x(0) = 0 \text{ m}$, $e_y(0) = 3 \text{ m}$, $e_\theta(0) = 0 \text{ rad}$,
- (iii) initial velocity of the robot: $v_c(0) = 1 \text{ m/sec}$, $\omega_c(0) = 0 \text{ rad/sec}$.



(a) for a straight path



(b) for a circular path

Figure 5. Results of path tracking simulation: (a) for a straight path; (b) for a circular path.



Figure 6. Prototype of an autonomous wheeled mobile robot (LCAR).

The simulation results show that all trajectories are smoothly approaching the given path with different values of the landing parameter c_x and the rate of convergence increases as the landing coefficient increases.

In order to investigate the tracking performance for a more general case, the simulations were repeated for a circular path. The simulation conditions were identical to those of the previous case except that $\omega_t = 0.2$ rad/sec. The results are given in Figure 5(b) which shows the proposed method has a fast convergence with smooth tracking motion even for the circular type path.

4.2. EXPERIMENTS

In order to test whether the proposed algorithm works practically in the commercial embedded system, the experiments are made for a prototype mobile robot, LCAR, with differential drive [17] as shown in Figure 6. The mechanical dimensions of the robot are $r_w = 0.1$ m and $d_w = 0.55$ m. The path tracking control algorithm is implemented in C and successfully performed by sampling time $\Delta T = 20$ m sec. The S/W program for path tracking is composed of the path planner, path error calculator, landing curve generator, and the bang-bang control part, as shown in Figure 7.

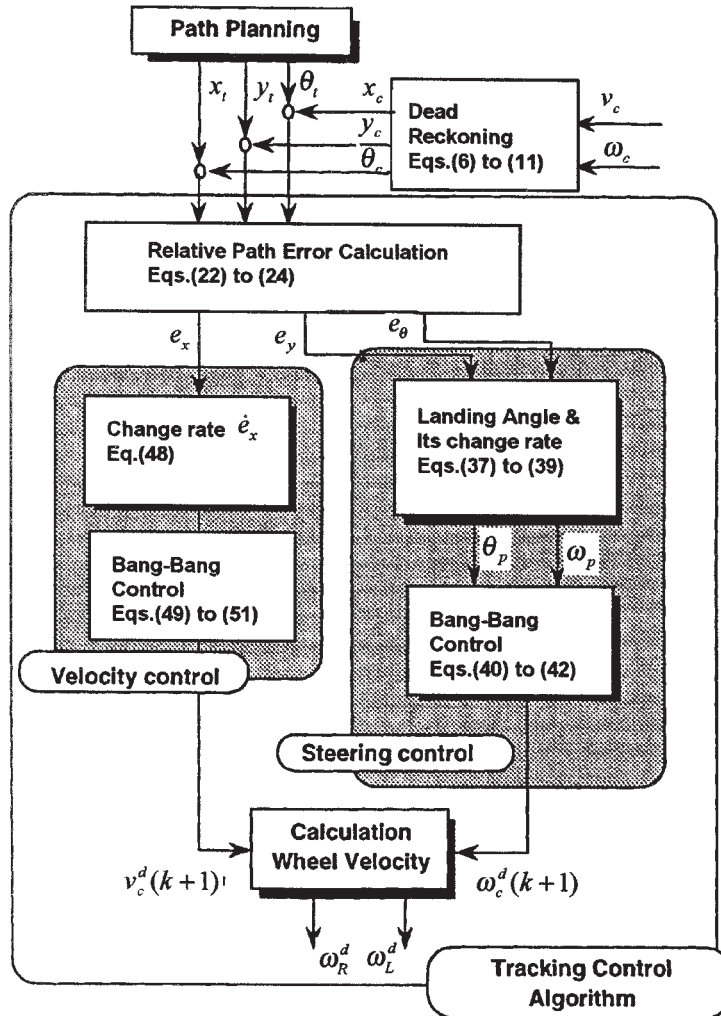


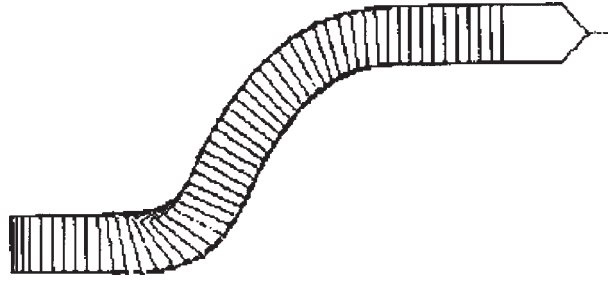
Figure 7. S/W implementation of the proposed algorithm.

Target vehicle generation. For the given path with the reference driving speed on the path, the target posture $\mathbf{P}_t(k)$ and target velocities $\mathbf{V}_t(k)$ are determined by (16)–(19).

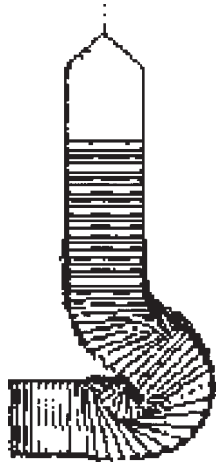
Dead reckoning. The current posture of the mobile robot $\mathbf{P}_c(k)$ and current velocities $\mathbf{V}_c(k)$ are computed by dead reckoning of (6)–(11).

Path tracking control. The robot velocities ω_c^{k+1} and v_c^{k+1} at the next sampling time are computed by the proposed tracking control method of (37)–(42) and (48)–(51).

Inverse kinematics. Those values are converted to wheel commands by using the inverse of the kinematic equations of (1) and (2).



(a) lane change motion



(b) discontinuous turning motion

Figure 8. Results of path tracking experiment: (a) lane change motion; (b) discontinuous turning motion.

Wheel servo control. The actual wheel velocities are controlled by wheel servo controllers which are independently designed by local closed loops for the right and left wheel driving mechanisms. During simulations, the dynamic effects of the robot are neglected under the assumption that they can be taken care of by feedforward compensation in wheel servo loops [18]. The robots with the proposed path tracking controller show a smooth and quick path tracking performance even for great initial path error or a discontinuous path. Figure 8 shows two examples demonstrating the validity of the proposed scheme.

5. Concluding Remarks

In this paper, we present a path tracking algorithm for nonholonomic mobile robots based on bang-bang control. By introducing the concept of a virtual target vehicle in defining the path error, we formulate the path tracking as a target following problem. Consideration of acceleration bounds from dynamic constraints of the

mobile robot leads to the velocity and steering control laws based on the bang-bang control scheme. To overcome the nonholonomic constraints, the landing curve works as an intermediate path smoothly steering the rotation of the robot towards the reference path. The convergence of the proposed scheme and conditions for the design parameter are analytically discussed using the Lyapunov method. The proposed tracking algorithm is not strictly time-optimal since each control law is separately considered to cope with the nonholonomic problem which makes it impossible to design the time-optimal path tracking controller. A little sacrifice of optimality leads, however, to the real-time tracking algorithm guaranteeing the smooth tracking performance action. The smooth tracking nature of proposed tracking path control enables us to plan the path by simple methods using straight line or circular segments. A series of computer simulations shows that the proposed tracking algorithm is valid and effective for stable and consistent tracking motion. The proposed algorithm has been successfully applied to the real control system of LCAR robot and showed a satisfactory tracking function.

Appendix

In the appendix, we discuss the convergence of the proposed path tracking via Lyapunov approach. We first investigate the convergence of the bang-bang controller and next look into the proposed tracking algorithm.

A. PROOF OF STABILITY OF BANG-BANG CONTROLLER

When the position and velocity errors between the target and the mobile robot, e and \dot{e} , are defined as follows:

$$e = x_c - x_t, \quad (52)$$

$$\dot{e} = v_t - v_c. \quad (53)$$

In order to show that the control law of Equation (28) makes the phase domain, (e, \dot{e}) reach the switching curve from any initial condition $(e(0), \dot{e}(0))$, a Lyapunov function V_1 is defined as

$$V_1 = \frac{1}{2}e^2 + \frac{1}{2}\dot{e}^2, \quad (54)$$

and the first derivative becomes

$$\dot{V}_1 = e\dot{e} + \dot{e}\ddot{e}. \quad (55)$$

From the equation of the switching curve the error dynamics yields

$$\dot{e} = -(2a_{\max}|e|)^{1/2}\text{sgn}(e), \quad (56)$$

$$\ddot{e} = -a_t + a_{\max}\text{sgn}(e), \quad (57)$$

where a_t is the acceleration of the target. Substituting the above equations into Equation (55) results in

$$\dot{V}_1 = -(2a_{\max}|e|)^{1/2} \text{sgn}(e)(e + a_t + a_{\max}) < 0, \quad (58)$$

since $e \text{sgn}(e) \geq 0$ and $\text{sgn}(e)(a_t + a_{\max} \text{sgn}(e)) > 0$ if $|a_t| < a_{\max}$. Thus, the bang-bang controller is asymptotically stable, i.e., (e, \dot{e}) converges to the origin if the magnitude of a_t is bounded by a_{\max} .

B. CONVERGENCE OF THE PROPOSED TRACKING CONTROLLER

Since the driving velocity controller of Equations (49) through (51) is designed on the basis of the bang-bang controller, the stability of the bang-bang controller means that the tangential path error e_x converges to zero. On the other hand, in order to show that e_y and e_θ converge to zero by the steering control law given by Equations (40)–(42), another Lyapunov function is defined by

$$V_2 = \frac{1}{2}e_y^2 + \frac{1}{2}e_\theta^2, \quad (59)$$

and the derivative of Equation (59) becomes

$$\dot{V}_2 = e_y \dot{e}_y + e_\theta \dot{e}_\theta = e_y(v_c \sin(e_\theta) - \omega_t e_x) + e_\theta(\omega_t - \omega_c). \quad (60)$$

Assuming $\theta_c \rightarrow \theta_p$ to be guaranteed by the bang-bang control, and e_x eventually approaches to zero by the tangential velocity control, the first term of Equation (60) can be rewritten using Equation (39) as follows:

$$e_y \dot{e}_y = e_y v_c \sin(\theta_t - \theta_p) = \frac{-e_y v_c \tan(\theta_p - \theta_t)}{(1 + \tan^2(\theta_p - \theta_t))^{1/2}}. \quad (61)$$

Substituting Equation (37) into Equation (61) results in

$$e_y \dot{e}_y = \frac{-3e_y v_c c_x (e_y/c_x)^{2/3} \text{sgn}(e_y)}{(1 + \tan^2(\theta_p - \theta_t))^{1/2}} < 0 \quad (62)$$

since $c_x > 0$ and $v_c e_y \text{sgn}(e_y) > 0$ if $v_c > 0$ and $e_y \neq 0 > 0$. Also, applying Equation (38) to the second term of (60) with assumptions of $\omega_c \rightarrow \omega_p$ which is guaranteed by the bang-bang control law of (40), the result becomes

$$e_\theta \dot{e}_\theta = e_\theta(\omega_t - \omega_p) = -2e_\theta v_c \sin(e_\theta) \left(\frac{e_y}{c_x}\right)^{1/3} \frac{\text{sgn}(e_y)}{1 + \tan^2(\theta_p - \theta_t)} < 0 \quad (63)$$

since

$$\left(\frac{e_y}{c_x}\right)^{-1/3} \text{sgn}(e_y) > 0 \quad \text{if } e_y \neq 0 \quad \text{and} \quad e_\theta \sin(e_\theta) > 0 \quad \text{if } 0 < |e_\theta| < \pi/2.$$

From the results of Equations (62) and (63), $\dot{V}_2 < 0$ for $e_y e_\theta \neq 0$ and $\dot{V}_2 = 0$ for $e_y = 0$ and $e_\theta = 0$. Note that the conditions of $v_c > 0$ and $|e_\theta| < \pi/2$ were assumed during the proof of the convergence. This means the tracking algorithm is valid only under conditions that the robot have nonzero tangential velocity and its direction be guided by the landing curve guaranteeing $|e_\theta| < \pi/2$. This is common to nonholonomic vehicles.

References

1. Astolfi, A.: Discontinuous control of nonholonomic systems, *Systems Control Lett.* **27** (1996), 37–45.
2. Bloch, A. M. and McClamroch, N. H.: Control and stabilization of nonholonomic dynamic systems, *IEEE Trans. Automatic Control* **37**(11) (1992), 1746–1757.
3. Borenstein and Koren, Y.: Motion control analysis of a mobile robot, *ASME J. Dynamic Systems Meas. Control* **109** (1987), 73–79.
4. Cox, I. J.: Blanche – An experiment in guidance and navigation of an autonomous robot, *IEEE Trans. Robotics Automat.* **7**(2) (1991), 193–204.
5. Crowley, J.: Asynchronous control of orientation and displacement in robotic vehicles, in: *Proc. of the IEEE Internat. Conf. on Robotics and Automation*, 1989, pp. 1277–1282.
6. DeSantis, R. M.: Modeling and path-tracking control of a mobile wheeled robot with a differential drive, *Robotica* **13** (1995), 401–410.
7. Elnagar, A. and Basu, A.: Piecewise smooth and safe trajectory planning, *Robotica* **12** (1994), 299–307.
8. Feng, D. and Krogh, B. H.: Dynamic steering control of conventionally steered mobile robots, *J. Robotic Systems* **8**(5) (1991), 699–721.
9. Garcia-Cerezo, A., Ollero, A., and Martinez, J. L.: Design of a robust high-performance fuzzy path tracker for autonomous vehicles, *Internat. J. Systems Sci.* **27**(8) (1996), 799–806.
10. Guldner, J. and Utkin, V.: Tracking the gradient of artificial potential fields: Sliding mode control for mobile robots, *Internat. J. Control* **63**(3) (1996), 417–432.
11. Hemami, A., Mehrabi, M. G., and Cheng, R. M.: A new strategy for tracking in mobile robots and AGV's, in: *Proc. of the IEEE Internat. Conf. on Robotics and Automation*, 1990, pp. 1122–1127.
12. Hemami, A., Mehrabi, M. G., and Cheng, R. M.: Synthesis for an optimal control law for path tracking in mobile robots, *Automatica* **28**(2) (1992), 383–387.
13. Hemami, A., Mehrabi, M. G., and Cheng, R. M.: Optimal kinematic path tracking control of mobile robots with front steering, *Robotica* **12** (1994), 563–568.
14. Jiang, Z. and Nijmeijer, H.: Tracking control of mobile robots: A case study in backstepping, *Automatica* **33**(7) (1997), 1393–1399.
15. Kanayama, Y., Kimura, Y., Miyazaki, F., and Noguchi, T.: A stable tracking control method for an autonomous mobile robots, in: *Proc. of the IEEE Internat. Conf. on Robotics and Automation*, 1990, pp. 384–389.
16. Kanayama, Y. and Miyake, N.: Trajectory generation for mobile robots, in: *Proc. of the Internat. Symp. on Robotics Research*, 1985, pp. 333–340.
17. Koh, K. C. and Cho, H. S.: A path tracking control system for autonomous mobile robots: An experimental investigation, *Mechatronics* **4**(8) (1994), 799–820.
18. Koh, K. C. and Cho, H. S.: Wheel servo control based on feedforward compensation for an autonomous mobile robot, in: *Proc. of the IEEE Internat. Workshop on Intelligent Robotics and Systems*, 1995, pp. 454–459.
19. Komoriya, K., Tach, S., and Tanie, K.: A method of autonomous locomotion for mobile robots, *Advanced Robotics* **1**(1) (1989), 3–19.

20. Lee, S. S. and Williams, J. H.: A fast tracking error control method for an autonomous mobile robot, *Robotica* **11** (1993), 209–215.
21. Nelson, W. L.: Continuous steering-function control of robot cart vehicles, *IEEE Trans. Industrial Electronics* **36**(3) (1989), 330–337.
22. Ollero, A. and Heredia, G.: Stability Analysis of Mobile Robot Path Tracking, in: *Proc. of the IEEE Internat. Workshop on Intelligent Robotics and Systems*, 1995, pp. 491–496.
23. Reister, D. B. and Pin, F. G.: Time-optimal trajectories for mobile robots with two independently driven wheels, *Int. J. Robotics Res.* **13**(1) (1994), 38–54.
24. Singh, S. J. and Shin, D. H.: Position based path tracking for wheeled mobile robots, in: *Proc. of the IEEE Internat. Workshop on Intelligent Robotics and Systems*, 1989, pp. 386–391.
25. Tounsi, M. and Le Corre, J. F.: Trajectory generation for mobile robots, *Mathematics and Computers in Simulation*, 1996, pp. 367–376.
26. Tsugawa, S. and Murata, S.: Steering control algorithm for autonomous vehicle, in: *Proc. of the Japan-USA Symp. on Flexible Automation*, 1990, pp. 143–146.